Neurobiology of Disease

$G\alpha_{olf}$ Mutation Allows Parsing the Role of cAMP-Dependent and Extracellular Signal-Regulated Kinase-Dependent Signaling in L-3,4-Dihydroxyphenylalanine-Induced Dyskinesia

Cristina Alcacer,[1,2,3] Emanuela Santini,[4] Emmanuel Valjent,[1,2,3,5] Florence Gaven,[1,2,3,5] Jean-Antoine Girault,[1,2,3] and Denis Hervé[1,2,3]

[1]Inserm UMR-S 839, F-75005 Paris, France, [2]Institut du Fer à Moulin, F-75005 Paris, France, [3]Université Pierre et Marie Curie, F-75005 Paris, France, [4]Center for Neural Science, New York University, New York, New York 10003, and [5]Institut de Génomique Fonctionnelle, Department of Neurobiology, Inserm UMR-S 661, CNRS UMR 5203, Montpellier University I and II, F-34094 Montpellier cedex 05, France

Although L-3,4-dihydroxyphenylalanine (L-DOPA) remains the reference treatment of Parkinson's disease, its long-term beneficial effects are hindered by L-DOPA-induced dyskinesia (LID). In the dopamine (DA)-denervated striatum, L-DOPA activates DA D_1 receptor (D_1R) signaling, including cAMP-dependent protein kinase A (PKA) and extracellular signal-regulated kinase (ERK), two responses associated with LID. However, the cause of PKA and ERK activation, their respective contribution to LID, and their relationship are not known. In striatal neurons, D_1R activates adenylyl-cyclase through $G\alpha_{olf}$, a protein upregulated after lesion of DA neurons in rats and in patients. We report here that increased $G\alpha_{olf}$ levels in hemiparkinsonian mice are correlated with LID after chronic L-DOPA treatment. To determine the role of this upregulation, we performed unilateral lesion in mice lacking one allele of the *Gnal* gene coding for $G\alpha_{olf}$ ($Gnal^{+/-}$). Despite an increase in the lesioned striatum, $G\alpha_{olf}$ levels remained below those of unlesioned wild-type mice. In $Gnal^{+/-}$ mice, the lesion-induced L-DOPA stimulation of cAMP/PKA-mediated phosphorylation of GluA1 Ser845 and DARPP-32 (32 kDa DA- and cAMP-regulated phosphoprotein) Thr34 was dramatically reduced, whereas ERK activation was preserved. LID occurrence was similar in $Gnal^{+/+}$ and $Gnal^{+/-}$ mice after a 10-d L-DOPA (20 mg/kg) treatment. Thus, in lesioned animals, $G\alpha_{olf}$ upregulation is critical for the activation by L-DOPA of D_1R-stimulated cAMP/PKA but not ERK signaling. Although the cAMP/PKA pathway appears to be required for LID development, our results indicate that its activation is unlikely to be the main source of LID. In contrast, the persistence of L-DOPA-induced ERK activation in $Gnal^{+/-}$ mice supports its causal role in LID development.

Introduction

Parkinson's disease (PD) results from neurodegeneration of nigrostriatal dopamine (DA) neurons. Despite innovative therapies, the DA precursor L-3,4-dihydroxyphenylalanine (L-DOPA) remains the drug of reference. However, after an initial period of full efficacy, this treatment is complicated by L-DOPA-induced dyskinesia (LID) with an incidence of 30–50% after 5 years and 60% after 10 years (Rascol, 2000; Van Gerpen et al., 2006). Better understanding of the neuronal mechanisms underlying the development of LID is therefore important to identify therapeutic strategies (Cenci, 2007; Jenner, 2008).

DA D_1 receptor (D_1R) agonists are more efficient than D_2R agonists to induce dyskinesia in animal models and PD patients (Calon et al., 1999; Rascol et al., 2001, 2006; Carta et al., 2008). D_1Rs are necessary for LID development (Westin et al., 2007; Darmopil et al., 2009). D_1R signaling through cAMP-dependent protein kinase A (PKA) and 32 kDa DA- and cAMP-regulated phosphoprotein (DARPP-32) is activated by L-DOPA in 6-hydroxydopamine (6-OHDA)-lesioned rodents (Santini et al., 2007; Lebel et al., 2010) or MPTP-treated monkeys (Santini et al., 2010). Strong D_1R-dependent activation of extracellular signal-regulated kinase (ERK) (Gerfen et al., 2002; Pavón et al., 2006; Santini et al., 2007, 2009b; Westin et al., 2007; Rylander et al., 2009) and mammalian target of rapamycin (mTOR) signaling (Santini et al., 2009a) is also observed in striatonigral medium-sized spiny neurons (MSNs). Pharmacological or genetic blockade of these pathways supports their necessary role in LID (Santini et al., 2007, 2009a; Bateup et al., 2010; Fasano et al., 2010; Lebel et al., 2010). However, the cause of their

Received Feb. 21, 2012; accepted March 5, 2012.

Author contributions: C.A., E.S., E.V., J.-A.G., and D.H. designed research; C.A., E.S., E.V., F.G., and D.H. performed research; C.A., E.S., E.V., F.G., J.-A.G., and D.H. analyzed data; C.A., J.-A.G., and D.H. wrote the paper.

The work was supported by Inserm, Université Pierre et Marie Curie, and grants from the Fondation pour la Recherche Médicale, the Fondation pour la Recherche sur le Cerveau, European Research Council, the Michael Stem Parkinson's Research Foundation, and Agence Nationale de la Recherche Grant ANR09-MNPS-014. The Girault and Hervé group is affiliated to the Ecole des Neurosciences de Paris-Ile-de-France. The authors are grateful to Gilberto Fisone for his help, support, and comments on this manuscript. We thank Leonardo Belluscio for providing $Gnal^{+/-}$ mice, Sophie Longueville for genotyping, Natacha Roblot, Rachida Boukhari, and Yohann Bertelle for breading the mice, Charlotte Plestant for her help with image analysis, and the staff of the Institut du Fer à Moulin Imaging facility.

The authors declare no competing financial interests.

Correspondence should be addressed to Dr. Denis Hervé, Inserm, Unité Mixte de Recherche S839, Institut du Fer à Moulin, 17, rue du Fer à Moulin, F-75005 Paris, France. E-mail: denis.herve@inserm.fr.

DOI:10.1523/JNEUROSCI.0837-12.2012

 0270-6474/12/325900-11$15.00/0

activation in DA-deprived striatum and their relative contribution in LID development are unknown.

Levels of D_1R (Shinotoh et al., 1993; Turjanski et al., 1997; Hurley et al., 2001) and major mediators of D_1R signaling, including PKA and DARPP-32 (Girault et al., 1989; Nishino et al., 1993), are unchanged in PD and its animal models. In MSNs, D_1Rs and adenosine A_{2A} receptors ($A_{2A}Rs$) are coupled to adenylyl-cyclase through a heterotrimeric G-protein comprising $G\alpha_{olf}$, $G\beta2$, and $G\gamma7$ subunits (Drinnan et al., 1991; Hervé et al., 1993; Kull et al., 2000; Zhuang et al., 2000; Corvol et al., 2001; Schwindinger et al., 2003, 2010). Levels of $G\alpha_{olf}$ increase in DA-denervated striatum of rats and PD patients (Hervé et al., 1993; Marcotte et al., 1994; Penit-Soria et al., 1997; Corvol et al., 2004; Rangel-Barajas et al., 2011). Because $G\alpha_{olf}$ levels are a limiting factor for receptor signaling (Corvol et al., 2001, 2007), $G\alpha_{olf}$ upregulation is a plausible but untested mechanism for the D_1R hypersensitivity in LID-developing animals.

The objective of this study was to examine the association of $G\alpha_{olf}$ with LID and evaluate the respective contribution of cAMP- and ERK-mediated pathways in LID. We used a mouse model of hemiparkinsonism treated with L-DOPA (Lundblad et al., 2004) and heterozygous mutant mice lacking one allele of the $G\alpha_{olf}$ gene (*Gnal*) (Belluscio et al., 1998; Corvol et al., 2007). This approach allowed us to parse the role of these various signaling components in the apparition of LID.

Materials and Methods

Animals

We used 8-week-old C57BL/6J male mice. Mice heterozygous for a null mutation of the gene encoding $G\alpha_{olf}$ (*Gnal*) kindly provided by L. Belluscio (NINDS, NIH, Bethesda, MD) (Belluscio et al., 1998) were backcrossed for eight generations with C57BL/6J wild-type mice and mated with C57BL/6J mice for producing heterozygous *Gnal* mutant mice and wild-type littermates. Animals <30 weeks old were used for the experiments. The mice were maintained in a 12 h light/dark cycle, in stable conditions of temperature (22°C), with access to food and water *ad libitum*. All the experiments were in accordance with the guidelines of the French Agriculture and Forestry Ministry for handling animals (Decree 87-848) and were conducted under the approval of the Direction Départementale de la Protection des Populations de Paris (Authorization C-75-828, License B75-05-22).

6-OHDA lesions and postoperative care

Mice were anesthetized with a mixture of xylazine (10 mg/ml) and pentobarbital (25 mg/ml) (Centravet) and mounted in a digitalized stereotactic frame (Stoelting Europe) equipped with a mouse adaptor. 6-OHDA-HCl (3.0 mg/ml; Sigma-Aldrich) was dissolved in a solution containing 0.2 g/L ascorbic acid and 9 g/L NaCl. Mice received two unilateral injections (2×2 μl) of 6-OHDA into the right striatum at the following coordinates according to the mouse brain atlas of Paxinos and Franklin (2001): anteroposterior (AP), +1.2 mm; lateral (L), +2.1 mm; dorsoventral (DV), −3.2 mm; and AP, +0.6 mm; L, +2.4 mm; DV, −3.2 mm. Each injection was performed with a 36-gauge, 50-mm-long stainless steel cannula connected to a syringe pump (MTI Corporation) by a polyethylene catheter, at a slow rate of 0.25 μl/min to minimize tissue damage. After the injection, the cannula was left in place for an additional 4 min before being slowly retracted. Sham mice were injected with vehicle only (ascorbic acid in saline).

Postoperative care was needed to minimize the mortality rate. Mice were let on a warm plate during about 24 h after surgery to avoid hypothermia. To reduce suffering, mice received subcutaneous injections of a non-steroidal anti-inflammatory drug (flunixin meglumine, 4 mg/kg; Sigma-Aldrich), just after the surgery and twice daily during 2 d after surgery. All the lesioned mice were examined daily, and the weakest animals received injections of 5% sucrose (10 ml/kg, s.c.) and saline (10 ml/kg, i.p.) to avoid dehydration. Concentrated milk was provided to all the lesioned animals during 3 d after the operation. Mice were allowed to recover for 4 weeks before behavioral evaluation and drug treatment. Lesions were assessed at the end of experiments by determining the striatal levels of tyrosine hydroxylase (TH) using immunohistochemistry or immunoblotting (see below). Only animals with a TH-depleted area >80% of the striatum area and/or TH level reduction by >80% in the lesioned striatal area compared with the control side were included in the analyses (i.e., ~85% of surviving lesioned mice).

L-DOPA and benserazide treatments

L-DOPA and the peripheral DOPA decarboxylase inhibitor benserazide hydrochloride (Sigma-Aldrich) were dissolved together in physiological saline solution (9 g/L NaCl). L-DOPA and benserazide hydrochloride were injected intraperitoneally at a dose of 20 and 12 mg/kg, respectively, in a volume of 10 ml/kg body weight. For acute treatments, mice were killed 30 min after the first injection of L-DOPA and benserazide. The chronic treatment consisted in a daily single injection of L-DOPA and benserazide during 10 d. Mice were killed on day 11, 30 min after the last injection.

Behavioral tests

Cylinder test. On day 1 of chronic treatment, the anti-parkinsonian effects of L-DOPA on sensorimotor function were evaluated in the cylinder test (Lundblad et al., 2002). Each lesioned mouse was tested before the beginning of L-DOPA therapy and 1 h after the first injection of L-DOPA plus benserazide. Mice were placed one by one in glass cylinders (10 cm diameter and 15 cm height) and video recorded for 5 min without previous habituation to the glass cylinder. Once introduced into the cylinder, the mice showed an exploratory behavior reflected by rearing and forepaw contacts on the wall. The number of contacts with the right or left forepaw was counted in blind conditions regarding mouse genotype. To eliminate accidental touches without physiological meaning, we counted only contacts in which the animal supported its body weight on the paw with extended digits. The use of the impaired (left) forepaw was expressed as a percentage of the total number of contacts on the wall.

Abnormal involuntary movements. 6-OHDA-lesioned mice were chronically treated with L-DOPA for 10 d. Abnormal involuntary movements (AIMs) were assessed on day 5 (two experiments) and day 10 (all experiments) in blind conditions regarding mouse genotype, using a previously validated scale for scoring LID in mouse (Lundblad et al., 2004, 2005). Immediately after L-DOPA administration, mice were placed in separate cages, and abnormal movements were assessed for 1 min (monitoring period) every 20 min, over a period of 140 min. Abnormal movements, clearly distinct from natural stereotyped behaviors (i.e., grooming, sniffing, rearing, and gnawing), were classified into four different subtypes: locomotive (tight contralateral turns), axial (contralateral dystonic posture of the neck and upper body), limb (jerky and fluttering movements of the limb contralateral to the side of the lesion), and orofacial (vacuous jaw movements and tongue protrusions) AIMs. Each subtype was scored on a severity scale from 0 to 4: 0, absent; 1, occasional; 2, frequent; 3, continuous; 4, continuous and not interruptible by external stimuli. The total AIMs score corresponded to the sum of individual scores for each AIM subtype. A composite score was obtained by the addition of scores for axial, limb, and orofacial AIMs (ALO score). The ALO score is considered to more closely reflect the human dyskinetic behavior than the locomotive AIMs score (LOC score) (Lundblad et al., 2002). To identify the extreme behaviors, highly and weakly dyskinetic mice were separated by a quartile analysis based on total AIMs scores.

Tissue preparation and immunofluorescence

Thirty minutes after the last injection of L-DOPA, mice were rapidly anesthetized with pentobarbital (500 mg/kg, i.p.; Sanofi-Aventis) and perfused transcardially with 40 g/L paraformaldehyde in PBS (0.1 M sodium phosphate, 0.14 M NaCl), pH 7.4. Brains were postfixed overnight in the same solution at 4°C. The following day, 30-μm-thick sections were cut with a Vibratome (Leica) and stored at −20°C in a buffered solution containing 30% (v/v) ethylene glycol, 30% (v/v) glycerol, and 0.1 M sodium phosphate, pH 7.4, until they were processed for immunofluorescence. Brain regions were identified using a mouse brain atlas (Paxinos and Franklin, 2001), and sections at +0.86 mm from bregma (dorsal striatum) were selected and processed as follows.

Day 1. Free-floating sections were rinsed in Tris-buffered saline (TBS) (0.10 M Tris, 0.14 M NaCl), pH 7.4, incubated for 5 min in TBS containing

3% H_2O_2 (v/v) and 10% methanol (v/v), and rinsed three times 10 min in TBS. After 20 min incubation in 0.2% Triton X-100 in TBS (v/v), sections were rinsed three times in TBS, blocked with 30 g/L BSA in TBS, and incubated overnight (or longer as indicated) at 4°C with the primary antibodies. For detection of phosphorylated proteins, 0.1 M NaF was included in all buffers and incubation solutions. Antibodies were a mouse monoclonal antibody for TH (1:500 with an incubation ≥ 2 d; Sigma-Aldrich), a rabbit polyclonal antibody for $G\alpha_{olf}$ protein (1:500) (Hervé et al., 2001), rabbit polyclonal antibodies for phospho-Thr202/Tyr204–ERK1/2 (phospho-ERK, 1:400; Cell Signaling Technology), phospho-Ser10-acetyl-Lys14-histone H3 (pAcH3) (1:500; Millipore), and phospho-(Ser/Thr) PKA substrate (phospho-PKA substrate, 1:500; Cell Signaling Technology).

Day 2. After incubation with primary antibodies, sections were rinsed three times for 10 min in TBS and incubated for 45 min with goat Cy3-coupled (1:400; The Jackson Laboratory) or goat Alexa Fluor 488-coupled (1:400; Invitrogen) secondary antibodies. Finally, sections were rinsed for 10 min twice in TBS and twice in Tris buffer (0.25 M Tris, pH 7.4) before mounting in Vectashield (Vector Laboratories). For immunofluorescence detection with Odyssey–LI-COR infrared fluorescent detection system (see below), suitable secondary antibodies were used: IRDye 700DX-conjugated anti-rabbit IgG and IRDye 800CW-conjugated anti-mouse IgG (Rockland Immunochemical), diluted in TBS (1:1000). After rinsing as above, sections were mounted on glass slides and dried for 2 h. For determining the TH-depleted area in the lesioned mice, TH immunoreactivity was revealed by immunohistochemistry using biotinylated antibodies, avidin–biotin–peroxidase complex (Vector Laboratories), and 3,3′-diaminobenzidine staining (Valjent et al., 2004).

Confocal microscopy analysis of brain sections

Confocal microscopy and image analysis were performed at the Institut du Fer à Moulin imaging facility. Images from each region of interest were obtained with a sequential laser-scanning confocal microscope (SP5; Leica) using the same adjustments for all the sections from one experiment. The number of phospho-ERK-positive cells was counted manually in 375 × 375 μm confocal images taken in the lesioned and unlesioned dorsolateral striatum in blind conditions concerning the mouse genotype. MacBiophotonics Image J was used to count automatically the number of nuclei positive for pAcH3 and phospho-PKA substrate. TH and $G\alpha_{olf}$ immunofluorescence intensity was quantified in the striatum with MacBiophotonics Image J, and the data represented mean gray levels above background value in 375 × 375 μm confocal images. The background level was evaluated by measuring the mean gray values in large fiber bundles passing through the striatum. All measurements were performed in blind conditions regarding the mouse treatment and genotype.

LI-COR analysis of brain sections

In some experiments, TH, $G\alpha_{olf}$, and pAcH3 immunofluorescence intensity was measured using the Odyssey–LI-COR infrared fluorescent detection system (LI-COR). This system commonly used to quantify immunoblots can also be used to quantify immunofluorescence in regions of interest of tissue sections. All sections were scanned together at 21 μm resolution. The regions of interest were drawn as a circle of 1.0 mm diameter in the dorsolateral striatum on the lesioned and unlesioned sides. The mean fluorescence intensity was measured in the regions of interest, and the background was determined in the cerebral cortex, a non-immunoreactive region. The validity of this approach to evaluate $G\alpha_{olf}$ levels was tested by determining the relationship between the fluorescence intensity and the amount of striatal tissue. Samples containing increasing amounts of $G\alpha_{olf}$ were prepared by mixing extracts [10 mg/ml protein in 2% (w/v) SDS] of striatum and cortex that expresses and does not express $G\alpha_{olf}$, respectively. Two microliters of these samples were spotted on nitrocellulose membrane (Hybond ECL; GE Healthcare). After fixation in a Ponceau S solution (Sigma-Aldrich), the membrane was blocked in BSA (30 g/L in TBS) and incubated in anti-$G\alpha_{olf}$ primary and IRDye-conjugated anti-rabbit secondary antibodies as described above. The mean fluorescence intensity of each dot was measured using the Odyssey–LI-COR detection system, and the background was determined as the fluorescence intensity of the dots containing only cortex extract. In parallel, free-floating brain sections were incubated in the same solutions as the nitrocellulose membrane, and mean fluorescence intensity was measured in various striatal areas as described above. Results of quantification with Odyssey-LI-COR were expressed as arbitrary units within each experiment.

Immunoblotting

Mice were killed by decapitation 30 min after L-DOPA plus benserazide injection. The heads of the animals were immediately immersed in liquid nitrogen for 6 s. The brains were removed, and the striata were dissected out within 20 s on an ice-cold surface, sonicated in 750 μl of 10 g/L SDS, and placed at 100°C for 10 min. This extraction procedure has been previously shown effective in preventing protein phosphorylation and dephosphorylation, hence ensuring that the level of phosphoproteins measured *ex vivo* reflects the *in vivo* situation (Svenningsson et al., 2000). Aliquots (5 μl) of the homogenate were used for protein determination using a bicinchoninic acid assay kit (Pierce Europe). Equal amounts of protein (20 μg) were separated by 10% (w/v) PAGE in the presence of SDS and transferred overnight to polyvinylidene difluoride membranes (GE Healthcare) (Towbin et al., 1979). The membranes were immunoblotted using phospho-Ser845 (Cell Signaling Technology) and phosphorylation state-independent (Millipore) glutamate AMPA receptor subunit 1 (GluA1) antibodies, phospho-Thr34 rabbit polyclonal and phosphorylation state-independent mouse monoclonal DARPP-32 antibodies (both gifts from P. Greengard, Rockefeller University, New York, NY), and TH monoclonal mouse antibodies (Millipore). Secondary antibodies (1:5000) were IRDye 700DX-conjugated anti-rabbit IgG and IRDye 800CW-conjugated anti-mouse IgG (Rockland Immunochemical). Their binding was quantified using an Odyssey–LI-COR infrared fluorescent detection system (LI-COR). The levels of phosphoproteins were normalized for the amount of the corresponding total protein detected in the sample.

Statistics

Correlations between variables were estimated using multiple regression analysis. Multiple comparisons were analyzed using two-way ANOVA, followed by Bonferroni's *post hoc* tests for specific comparisons. For two-group comparisons, two-tailed paired or unpaired Student's *t* test was used.

Results

$G\alpha_{olf}$ is upregulated in the 6-OHDA-lesioned dorsolateral mouse striatum

Increased $G\alpha_{olf}$ protein levels have been reported in the dorsal striatum of 6-OHDA-lesioned rats (Hervé et al., 1993; Marcotte et al., 1994; Penit-Soria et al., 1997; Corvol et al., 2004; Rangel-Barajas et al., 2011) and in the putamen of PD patients (Corvol et al., 2004). In contrast, $G\alpha_{olf}$ levels after DA depletion had never been explored in the hemiparkinsonian mouse model. In a first experiment, we investigated the levels of $G\alpha_{olf}$ in the dorsal striatum of 6-OHDA-lesioned mice. Twelve mice (55% of the operated mice) survived and were well lesioned (for criteria, see Materials and Methods). We evaluated the lesion-induced changes in $G\alpha_{olf}$ and other markers in striatal sections using two different methods of immunofluorescence measurement with either the Odyssey–LI-COR system (Fig. 1*A–D*) or confocal microscopy (Fig. 1*E*, *F*).

The striatal 6-OHDA injections induced a dramatic decrease in TH immunofluorescence detected with Odyssey–LI-COR (Fig. 1*A*). TH immunoreactivity consistently disappeared in the most dorsolateral part of the striatum, although the lesion extension in the medioventral part varied from one animal to another. To detect the precise area of D_1R hypersensitivity within the striatum and to measure the levels of $G\alpha_{olf}$ specifically in this region, we used the L-DOPA-induced increase in pAcH3, a prominent response directly linked to D_1R hypersensitivity (Santini et al., 2009b; Cenci and Konradi, 2010). Lesioned mice were treated with L-DOPA (20 mg/kg) and benserazide (12 mg/kg) 30 min before being killed, a treatment that does not alter $G\alpha_{olf}$ levels

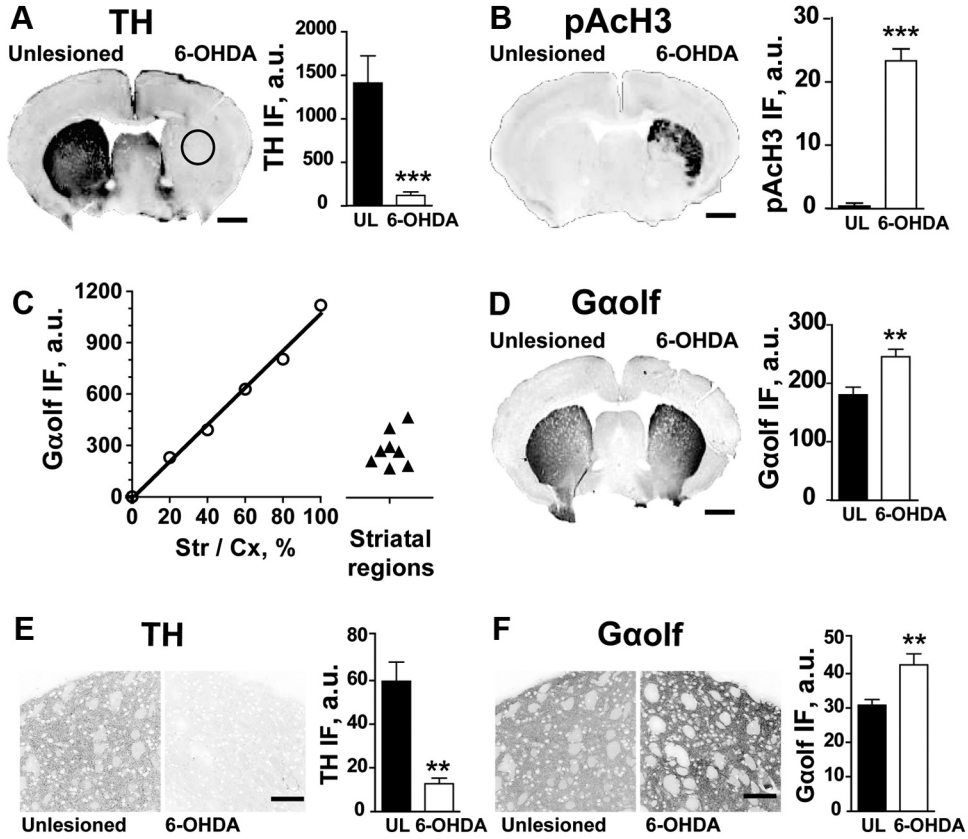

Figure 1. Unilateral 6-OHDA lesion increases $G\alpha_{olf}$ levels in the dorsal striatum. Immunoreactivity was detected using Odyssey–LI-COR system (***A–D***) or confocal microscope (***E***, ***F***). ***A***, ***B***, ***D***, Serial coronal brain sections from a mouse that received a unilateral 6-OHDA injection into the right striatum. ***A***, TH immunofluorescence (TH IF). ***B***, pAcH3 immunofluorescence (pAcH3 IF) showing the extent of signaling hypersensitivity in the dorsolateral part of the lesioned striatum. ***C***, Plot of $G\alpha_{olf}$ immunofluorescence quantification with Odyssey–LI-COR, as a function of the proportion of $G\alpha_{olf}$ protein in a dot blot assay. The samples were obtained by mixing various proportions of protein extracts from striatum (Str) expressing $G\alpha_{olf}$ and cortex (Cx) devoid of $G\alpha_{olf}$. The immunofluorescence values were determined in parallel in two regions of the striatum, in two brain sections (i.e., non-homogenized striatal slices; right, Striatal regions). These values were within the linear range of the standard curve. ***D***, $G\alpha_{olf}$ immunofluorescence (Gαolf IF). Quantification of mean immunofluorescence intensity (IF) on the unlesioned (UL) and lesioned (6-OHDA) sides is shown in ***A***, ***B***, and ***D*** in the dorsolateral part of the striatum (circled region of interest drawn in ***A***). Data are means ± SEM ($n = 11–13$). Paired two-tailed Student's *t* test: TH, $t = 4.57$; pAcH3, $t = 12.8$; $G\alpha_{olf}$, $t = 4.00$. Scale bar, 1 mm. ***E***, ***F***, Single confocal sections in the dorsolateral striatum showing TH (***E***) and $G\alpha_{olf}$ immunofluorescence (***F***). Data are means ± SEM ($n = 8–12$). Paired two-tailed Student's *t* test: TH, $t = 4.47$; $G\alpha_{olf}$, $t = 3.19$. Scale bar, 100 μm. $^{**}p < 0.01$, $^{***}p < 0.001$. a.u., Arbitrary units.

(Corvol et al., 2004; C.A. and D.H., unpublished observations), and the distribution of pAcH3-positive cells was determined in the striatum (Fig. 1*B*). An intense pAcH3 signal was detected in response to L-DOPA treatment in the dorsolateral part of the TH-depleted striatum (Fig. 1*B*). Interestingly, the area of strong pAcH3 immunoreactivity was consistently more restricted than the TH-depleted zone (Fig. 1*A*,*B*).

To validate the use of Odyssey–LI-COR for evaluating $G\alpha_{olf}$ levels in tissue, we compared immunofluorescence signals measured in striatal sections with those obtained with various concentrations of striatal homogenates in dot blot (Fig. 1*C*). In dot blot, fluorescence intensity was linearly related with the concentration of striatal tissue (and thus of $G\alpha_{olf}$) on a wide scale. The $G\alpha_{olf}$ immunofluorescence that we detected in various striatal regions appeared within the linear range, showing the validity of this measurement to detect changes in $G\alpha_{olf}$ levels. Using this approach, $G\alpha_{olf}$ immunofluorescence was found to increase in the dorsolateral part of the striatum in which TH immunofluorescence was absent and pAcH3 was present (Fig. 1*D*). Very similar results were obtained using confocal microscopy (Fig. 1*E*,*F*). Because quantification of images from confocal microscope provided results similar to those with Odyssey–LI-COR, we used confocal imaging in the rest of the study. Thus, our results revealed a significant increase in $G\alpha_{olf}$ immunoreactivity within the DA-deficient region of the striatum of 6-OHDA-lesioned mice, coincident with the area of increased D_1R signaling.

Striatal $G\alpha_{olf}$ increase correlates with dyskinetic behavior

Because $G\alpha_{olf}$ immunoreactivity was higher in the mouse dorsolateral striatum after the lesion, we examined whether this increase was maintained after chronic treatment with L-DOPA and whether it was associated with the development of LID. To address this question, 6-OHDA-lesioned mice received a 10 d treatment with L-DOPA (20 $mg \cdot kg^{-1} \cdot d^{-1}$) and benserazide (12 mg/kg) referred to as "L-DOPA" below. In a series of six experiments, 65 mice (68% of the operated mice) survived the operation and displayed a decrease in striatal TH levels >80%. One group received a single injection of L-DOPA ($n = 21$), and another group was chronically treated with L-DOPA during 10 d ($n = 44$). An additional control group of six sham-lesioned mice also received L-DOPA chronically. Thirty minutes after the last injection of L-DOPA, all the animals were killed to compare the $G\alpha_{olf}$ levels in their 6-OHDA-injected and intact striata by confocal immunofluorescence analysis. For comparison between different animals and experiments, we used the immunofluorescence on the lesioned side/immunofluorescence on the unlesioned side ratio (Fig. 2*A*). As expected, in the sham-operated mice, the $G\alpha_{olf}$ immu-

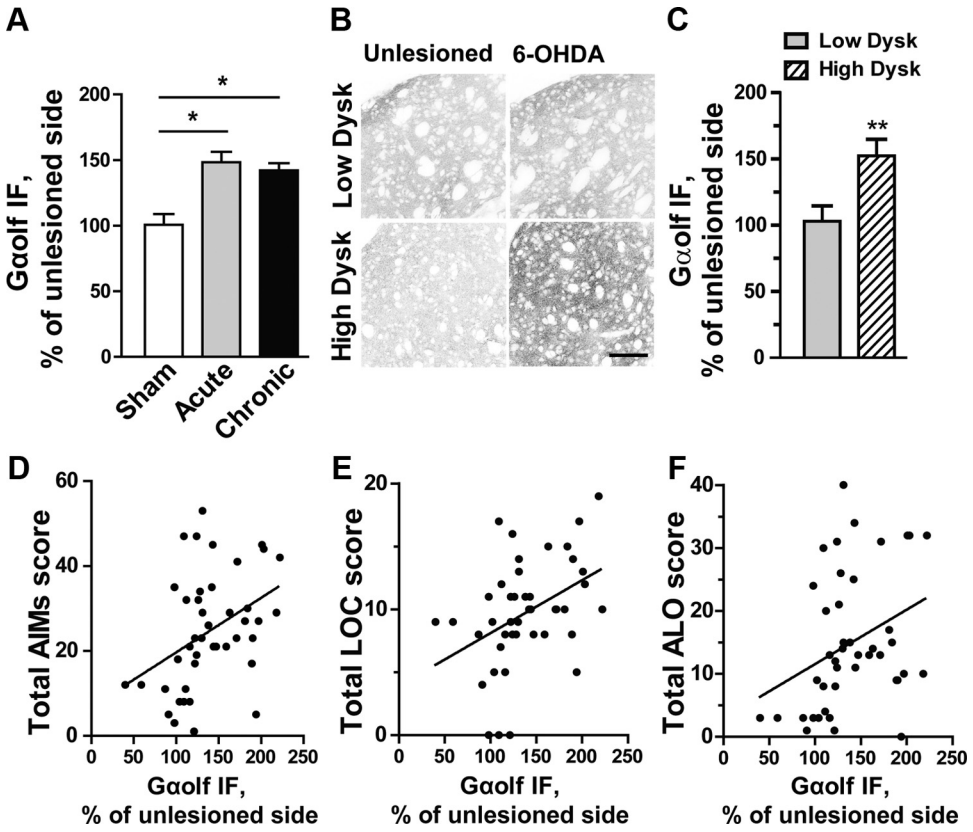

Figure 2. The increase in striatal $G\alpha_{olf}$ levels correlates with dyskinetic behavior. ***A***, Quantification of $G\alpha_{olf}$ immunofluorescence (IF) in the dorsal striatum of sham-operated mice treated with L-DOPA for 10 d (Sham; $n = 6$), 6-OHDA-lesioned mice treated with a single injection of L-DOPA (Acute; $n = 21$), or daily for 10 d (Chronic; $n = 44$). Data are expressed as percentage of the unlesioned (UL) side in each group and are means ± SEM. One-way ANOVA, $F_{(2,68)} = 4.16$, $^{*}p < 0.05$. *Post hoc* comparison (Bonferroni's test): $^{*}p < 0.05$ versus sham. ***B***, Comparison of $G\alpha_{olf}$ immunofluorescence in the unlesioned and 6-OHDA-lesioned striata of mice with low (Low Dysk, top row) and high (High Dysk, bottom row) scores of LID. Scale bar, 100 μm. ***C***, Comparison of $G\alpha_{olf}$ levels in the 25% 6-OHDA-lesioned chronically L-DOPA-treated mice in ***A*** that developed the weakest (total AIM score < 12.5; Low Dysk; $n = 11$) and strongest (>33.5; High Dysk; $n = 11$) dyskinesia. Data are means ± SEM. Unpaired two-tailed Student's *t* test: $t = 2.89$, $^{**}p < 0.01$. ***D–F***, Correlation between $G\alpha_{olf}$ levels and total AIMs (***D***) ($r = 0.40$, $F_{(1,42)} = 7.96$, $p < 0.01$), LOC AIMs (***E***) ($r = 0.41$, $F_{(1,42)} = 8.56$, $p < 0.01$), and ALO AIMs (***E***) ($r = 0.34$, $F_{(1,42)} = 5.38$, $p < 0.05$).

nofluorescence intensities were similar in the vehicle-injected and intact striata (Fig. 2*A*). In contrast, striatal $G\alpha_{olf}$ immunofluorescence was significantly higher in the 6-OHDA-lesioned striatum than in the contralateral striatum in mice that had received one or repeated injections of L-DOPA (Fig. 2*A*).

Because among chronically L-DOPA-treated mice some animals developed intense LID but not others, we examined whether the levels of $G\alpha_{olf}$ differed between these two groups. To perform this analysis, we separated the highly dyskinetic mice (i.e., those having total AIMs scores in the quartile of highest values, >33.5; $n = 11$) and the weakly dyskinetic mice (total AIMs score in the quartile of lowest values, <12.5; $n = 11$), among a total number of 44 animals. The mice in both groups displayed >80% reduction in TH in the dorsolateral striatum (data not shown). In the quartile of highly dyskinetic mice, $G\alpha_{olf}$ immunofluorescence was higher in the lesioned striatum than in the contralateral unlesioned striatum (Fig. 2*B*,*C*). In contrast, in the quartile of weakly dyskinetic mice, $G\alpha_{olf}$ immunofluorescence was similar on the two sides (Fig. 2*B*,*C*). We then examined whether there was a correlation between the levels of $G\alpha_{olf}$ and the intensity of AIMs, including all the lesioned animals that had received a chronic L-DOPA treatment. Although the experimental points appeared quite disperse, statistical analysis revealed a significant positive correlation between $G\alpha_{olf}$ immunofluorescence and the total AIMs score (Fig. 2*D*), the locomotor component of LID (LOC) (Fig. 2*E*), and the composite score of ALO AIMs (Fig. 2*F*), which have been suggested to be more similar to the human LID than the LOC AIMs (Lundblad et al., 2002). From these experiments, we concluded that the increase in $G\alpha_{olf}$ in the dorsolateral striatum of hemiparkinsonian mice was somehow associated with the severity of dyskinetic behavior. This result suggested a possible implication of $G\alpha_{olf}$ striatal upregulation in the development of LID in the mouse model of hemiparkinsonism.

Effects of 6-OHDA lesions on $G\alpha_{olf}$ in *Gnal*$^{+/-}$ mice

Given the positive correlation between $G\alpha_{olf}$ increases and dyskinesia, we used a genetic model in which $G\alpha_{olf}$ levels are decreased to examine the consequences of this reduction on LID and signaling responses. Homozygous $G\alpha_{olf}$ knock-out mice (*Gnal*$^{-/-}$) have a severe phenotype because of the combination of olfactory and striatal deficits (Belluscio et al., 1998; Zhuang et al., 2000; Corvol et al., 2001). These mice usually die in the early postnatal period and could not be used in our study. In contrast, *Gnal*$^{+/-}$ mice, which develop and breed normally, provide a very interesting model because they display a decrease of ~50% in $G\alpha_{olf}$ protein levels (Fig. 3*A*) and a 30–50% deficit in D_1R- or A_{2A}R-activated cAMP production *in vitro* when compared with wild-type littermates (Corvol et al., 2001, 2007). Because striatal $G\alpha_{olf}$ immunofluorescence was increased by ~50% in the lesioned striatum of dyskinetic mice whereas it was similar to the unlesioned tissue in weakly dyskinetic mice (Fig. 2*C*), *Gnal*$^{+/-}$ mice in which $G\alpha_{olf}$ was reduced but not absent were a good model for testing the specific implication of $G\alpha_{olf}$ upregulation.

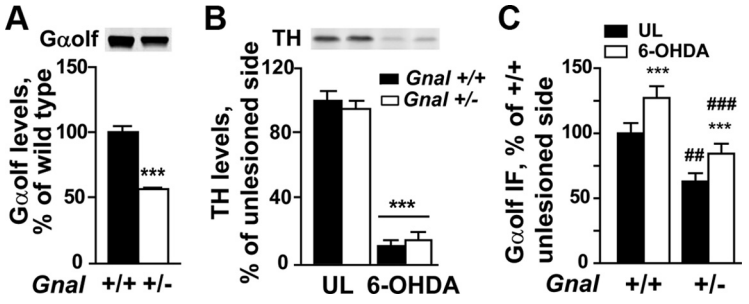

Figure 3. $G\alpha_{olf}$ and TH levels in 6-OHDA-lesioned *Gnal*$^{+/-}$ and control mice. ***A***, Quantification of $G\alpha_{olf}$ levels in mice heterozygous for a null mutation of *Gnal* gene (+/−) and their wild-type littermates (+/+) by immunoblotting. Data are expressed as percentage of the mean in wild-type mice and are means ± SEM ($n = 4–6$). Unpaired two-tailed Student's *t* test: $G\alpha_{olf}$ $t = 10.93$, ***$p < 0.0001$. ***B***, Quantification of TH levels by immunoblotting. Data are expressed as percentage of the means of unlesioned (UL) side of *Gnal*$^{+/+}$ mice and are means ± SEM ($n = 7–8$). Two-way ANOVA: effect of lesion, $F_{(1,24)} = 357$, $p < 0.0001$; effect of genotype, $F_{(1,24)} = 0.01$, not significant; interaction, $F_{(1,24)} = 0.90$, not significant. *Post hoc* comparison (Bonferroni's test): ***$p < 0.001$, 6-OHDA versus unlesioned (UL) for each genotype. ***C***, Quantification of $G\alpha_{olf}$ mean immunofluorescence (IF) intensity in 6-OHDA-lesioned *Gnal*$^{+/-}$ and wild-type control (+/+) mice chronically treated with L-DOPA. $G\alpha_{olf}$ immunofluorescence was measured in the dorsolateral striatum by confocal microscopy in three independent experiments for each mouse and normalized to the mean values in wild-type mice for each experiment. Two-way ANOVA analysis effect of the lesion, $F_{(1,18)} = 133$, $p < 0.0001$; effect of the genotype, $F_{(1,18)} = 13.97$, $p < 0.01$; interaction, $F_{(1,18)} = 1.81$, not significant. *Post hoc* comparison (Bonferroni's test): ***$p < 0.001$, 6-OHDA-lesioned versus unlesioned; $^{\#\#}p < 0.01$ and $^{\#\#\#}p < 0.001$, *Gnal*$^{+/-}$ versus *Gnal*$^{+/+}$.

Wild-type (*Gnal*$^{+/+}$) and heterozygous (*Gnal*$^{+/-}$) mice were lesioned with 6-OHDA and, after a 4 week recovery, treated with L-DOPA during 10 d (17 well-lesioned mice in each group survived the whole experimental procedure, corresponding to ~60% of operated mice). They were killed 30 min after the last L-DOPA injection, and proteins of interest were analyzed by immunofluorescence or immunoblotting. Immunoblotting showed that the two groups of mice displayed the same degree of TH reduction in their lesioned striatum, indicating that 6-OHDA had a similar ability to destroy DA innervation in the two genotypes (Fig. 3*B*). Immunohistochemistry indicated that the TH-depleted area was similar in wild-type and *Gnal*$^{+/-}$ mice (87 ± 2 and 92 ± 2% of the total striatum area, respectively; Student's *t* test, $t = 1.48$; DF = 18, not significant). To compare the changes in $G\alpha_{olf}$ immunofluorescence in mutant and wild-type mice, three sections from each animal were labeled and quantified using confocal imaging in three independent experiments, and the results were averaged (Fig. 3*C*). As expected, the levels of $G\alpha_{olf}$ detected with this method were lower in unlesioned striatum of mutant mice compared with wild type (Fig. 3*C*). Interestingly, $G\alpha_{olf}$ immunofluorescence levels in *Gnal*$^{+/-}$ mice were increased in the lesioned striatum when compared with the contralateral intact striatum (Fig. 3*C*). The relative increase on the lesioned side compared with the contralateral side was similar in the two genotypes (*Gnal*$^{+/+}$, 132 ± 5%; *Gnal*$^{+/-}$, 145 ± 6% of the contralateral side levels, mean ± SEM; Student's *t* test, $t = 1.6$; DF = 18, not significant). However, the levels of $G\alpha_{olf}$ immunofluorescence in the lesioned striatum of mutant mice remained below those in the intact striatum of wild-type mice (−16%; Fig. 3*C*). Similar results were observed using the Odyssey–LI-COR system (data not shown). Altogether these results showed that the mechanisms of $G\alpha_{olf}$ increase after 6-OHDA lesion were unaltered in heterozygous mutant mice but that the gene dosage effect maintained the levels of the protein below those in unlesioned wild-type mice.

Behavioral responses of hemiparkinsonian *Gnal*$^{+/-}$ mice are similar to wild type

During L-DOPA treatment, the 6-OHDA-lesioned *Gnal*$^{+/+}$ and *Gnal*$^{+/-}$ mice were evaluated in behavioral tests. Mice were first subjected to the cylinder test before (baseline) and after the first administration of L-DOPA. Before L-DOPA, *Gnal*$^{+/+}$ and *Gnal*$^{+/-}$ mice displayed a marked reduction in the usage of the forelimb contralateral to the lesion (Fig. 4*A*), reflecting the hypokinetic effects of 6-OHDA lesion. A similar recovery of the forelimb usage was observed in both genotypes 1 h after L-DOPA treatment. Thus, the anti-parkinsonian effect of L-DOPA appeared to be preserved in *Gnal*$^{+/-}$ mice.

At the end of the 10 d L-DOPA treatment, the animals were scored for the various types of AIMs. No significant difference was observed between *Gnal*$^{+/-}$ and *Gnal*$^{+/+}$ mice in axial, limb, and orofacial AIMs induced by chronic L-DOPA treatment, and the ALO composite score was not significantly changed in the mutant mice (Fig. 4*B*). Similarly, no significant difference in LOC score was observed between the two genotypes (Fig. 4*C*). The total AIMs score and the time course of L-DOPA effects were not significantly affected by *Gnal* haplodeficiency (Fig. 4*D*). We also compared LID in *Gnal*$^{+/-}$ and wild-type mice after only 5 d of L-DOPA treatment (Fig. 4*E*), and we detected no significant difference between the two genotypes, suggesting the absence of alteration in the LID development in *Gnal*$^{+/-}$ mice. Thus, our results clearly showed that the partial deficit in $G\alpha_{olf}$ in heterozygous mice did not change the incidence and intensity of LID after a 10 d treatment.

L-DOPA-induced cAMP-dependent phosphorylation is dramatically reduced in the lesioned striatum of *Gnal*$^{+/-}$ mice

We have reported previously a dissociated alteration of signaling pathways in *Gnal*$^{+/-}$ mice in response to psychostimulants *in vivo*, with markedly decreased cAMP-dependent phosphorylation and normal ERK signaling (Corvol et al., 2007). It was therefore particularly interesting to examine the signaling responses to L-DOPA in *Gnal*$^{+/-}$ mice. Because $G\alpha_{olf}$ is directly involved in the stimulation of cAMP/PKA signaling (Corvol et al., 2007), we compared the phosphorylation of several PKA substrates in chronically L-DOPA-treated *Gnal*$^{+/-}$ and wild-type mice. In *Gnal*$^{+/+}$ ($n = 9$) and *Gnal*$^{+/-}$ ($n = 11$) mice, we evaluated the number of neurons immunolabeled with an antibody recognizing the phosphorylated form of the PKA substrate consensus sequence, which has been validated for assessing the activity of cAMP/PKA pathway in neurons by immunofluorescence (Sindreu et al., 2007). A dramatic increase in the number of immunopositive neurons was observed after L-DOPA in the lesioned striatum of wild-type mice showing a strong responsiveness of cAMP/PKA signaling (Fig. 5*A*,*B*). This increase was significantly lower in the lesioned striatum of *Gnal*$^{+/-}$ mice, indicating a reduction of cAMP/PKA signaling in these mice. The persistence of some level of activation may correspond to a persistent partial PKA activation or to the reaction of the antibody with proteins phosphorylated by other kinases. Therefore, in a different set of lesioned animals, we examined by immunoblotting the phosphorylation of two well-characterized PKA substrates, AMPA receptor subunit GluA1 at Ser845 (Snyder et al., 2000) and DARPP-32 at Thr34 (Hemmings et al., 1984). Phosphorylation of these sites has been shown to be correlated with the occurrence of LID (Santini et

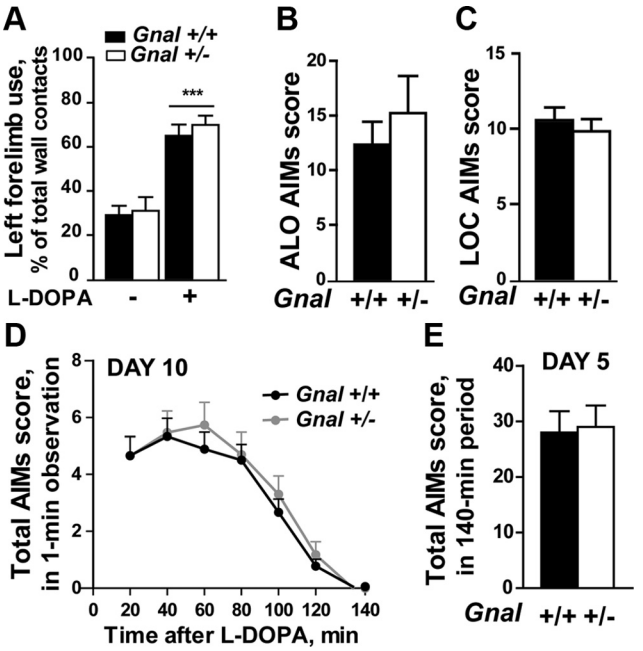

Figure 4. LID is not altered in *Gnal* heterozygous mice. Heterozygous (+/−) *Gnal* mutant and wild-type (+/+) mice were lesioned and treated with L-DOPA and benserazide during 10 d. ***A***, Forelimb use was determined using the cylinder test in the 6-OHDA-lesioned mice before (−) and after (+) administration of L-DOPA on the first day of treatment. Data are means ± SEM ($n = 7–8$). Repeated-measure ANOVA (with the within-subjects factor of treatment and the between-subjects factor of genotype): effect of treatment, $F_{(1,26)} = 56$, $p < 0.0001$; effect of genotype, $F_{(1,26)} = 0.49$, not significant; interaction between genotype and treatment, $F_{(1,26)} = 0.09$, not significant. *Post hoc* comparison (Bonferroni's test): ***$p < 0.001$, before versus after L-DOPA. ***B***, Sum of ALO AIMs scored during 140 min period after L-DOPA. Comparison between +/+ ($n = 18$) and +/− ($n = 23$) mice. Data are means ± SEM. Unpaired two-tailed Student's *t* test: $t = 0.62$, not significant. ***C***, Sum of LOC AIMs scored during 140 min period after L-DOPA in the same animals. Data are means ± SEM. Unpaired two-tailed Student's *t* test: $t = 0.61$, not significant. ***D***, Time course of total AIMs (sum of ALO and LOC AIMs) scored every 20 min over a period of 140 min after the last L-DOPA administration. Repeated-measures two-way ANOVA (with the within-subjects factor of time and the between-subjects factor of genotype): effect of genotype, $F_{(1,234)} = 0.18$, not significant; effect of time, $F_{(6,234)} = 71$, $p < 0.0001$; interaction, $F_{(6,234)} = 0.43$, not significant. ***E***, Total AIMs (sum of ALO and LOC AIMs) scored during 140 min period after L-DOPA on day 5 of L-DOPA treatment. Data are means ± SEM. Student's *t* test, $t = 0.181$, not significant.

al., 2007). In the lesioned striatum of *Gnal*$^{+/+}$ mice, L-DOPA treatment induced an increased phosphorylation of GluA1 and DARPP-32 when compared with the unlesioned striatum (Fig. 5*C–E*), in agreement with previous results (Santini et al., 2007). In contrast, these responses were absent in *Gnal*$^{+/-}$ mice for Ser845–GluA1 (Fig. 5*C*,*D*) and markedly diminished for Thr34–DARPP-32 (Fig. 5*C*,*E*). A slight increase in baseline DARPP-32 phosphorylation was observed in Gnal$^{+/-}$ mice, but it was not significant and of uncertain meaning given the variability in baseline DARPP-32 phosphorylation between animals. These results show that, after a chronic treatment with L-DOPA, *in vivo* activation of the cAMP/PKA phosphorylation pathway is severely altered in *Gnal*$^{+/-}$ mice, despite the relative increase in Gα_{olf} protein induced by the lesion compared with the unlesioned striatum.

L-DOPA-induced activation of the ERK pathway is preserved in the lesioned striatum of *Gnal*$^{+/-}$ mice

The second signaling pathway that has been reported to be strongly activated by L-DOPA in the lesioned striatum is the ERK cascade (Gerfen et al., 2002; Pavón et al., 2006; Santini et al., 2007; Westin et al., 2007). The activation of this pathway is D_1R dependent (Gerfen et al., 2002; Westin et al., 2007) and takes place in striatonigral MSNs, which express this receptor (Santini et al., 2009b), although prolonged L-DOPA treatment was found to activate ERK pathway in the small population of cholinergic interneurons (Ding et al., 2011). Thirty minutes after injection of L-DOPA, after a 10 d treatment, we observed a dramatic increase in the number of neurons immunofluorescent for the diphosphorylated active form of ERK1/2 (pERK) in the lesioned striatum compared with the unlesioned side in *Gnal*$^{+/+}$ mice (Fig. 6*A*). A similar response was observed in *Gnal*$^{+/-}$ mutant mice (Fig. 6*A*). We also analyzed the phosphorylation of ERK2 by immunoblotting and found no difference between the two genotypes (pERK2/total ERK2: +/+, unlesioned, 100 ± 4 and 6-OHDA, 142 ± 11; +/−, unlesioned, 102 ± 3 and 6-OHDA, 141 ± 6, means ± SEM; two-way ANOVA; lesion effect, $F_{(1,57)} = 42.1$, $p < 0.001$; genotype effect, $F_{(1,57)} = 0.01$, not significant; interaction $F_{(1,57)} = 0.03$, not significant). We then examined pAcH3 immunoreactivity that is known to be dependent on ERK activation and is strongly increased by L-DOPA in 6-OHDA-lesioned striatonigral MSNs (Santini et al., 2007, 2009b). A dramatic increase in the number of pAcH3-positive neurons was observed in the lesioned striatum of wild-type mice (Fig. 6*B*). A virtually identical response was observed in *Gnal*$^{+/-}$ mice (Fig. 6*B*). Thus, there was a marked contrast between the identical pERK responses to L-DOPA in *Gnal*$^{+/+}$ and *Gnal*$^{+/-}$ mice and the clear reduction in the PKA pathway response in *Gnal*$^{+/-}$ mice.

Because chronic treatment by L-DOPA may change the response of ERK pathway (Santini et al., 2007; Cenci and Konradi, 2010; Ding et al., 2011), we wondered whether this treatment could blunt differences between *Gnal*$^{+/+}$ and *Gnal*$^{+/-}$ mice. We therefore examined in a different batch of mice the responses to a single acute injection of L-DOPA. A very strong increase in pERK-positive (Fig. 6*C*) and pAcH3-positive (Fig. 6*D*) cells was observed in the lesioned striatum, and this effect was identical in wild-type and heterozygous *Gnal* mutant mice. These results clearly show that the decrease in Gα_{olf} did not alter ERK activation in response to L-DOPA.

Discussion

The present study addressed the involvement of Gα_{olf} upregulation in LID in a mouse model of hemiparkinsonism. The use of mice partially deficient in Gα_{olf} (*Gnal*$^{+/-}$) allowed us to determine its contribution to LID and to intracellular signaling cascades presumably involved in LID development or expression.

Gα_{olf} upregulation in dyskinetic mice

We replicated in mice the upregulation of Gα_{olf} protein observed in the dorsal striatum of hemiparkinsonian rats and PD patients (Hervé et al., 1993; Marcotte et al., 1994; Penit-Soria et al., 1997; Corvol et al., 2004; Rangel-Barajas et al., 2011). Previous data suggested that this upregulation was posttranscriptional (Hervé et al., 1993) and resulted from a lack of usage of the receptor (Hervé et al., 2001). Although its precise mechanisms are still unknown, a parallel can be made with the highly related Gαs whose degradation increases after its activation in cultured cells (Levis and Bourne, 1992). In support of this hypothesis, treatment of lesioned rats with L-DOPA or a D_1R agonist normalized Gα_{olf} levels (Corvol et al., 2004; Rangel-Barajas et al., 2011). However, Gα_{olf} increase was observed in the putamen of PD patients who had received a prolonged L-DOPA treatment (Corvol et al., 2004). The present study shows a correlation between LID and maintenance of increased Gα_{olf} levels. When the mice

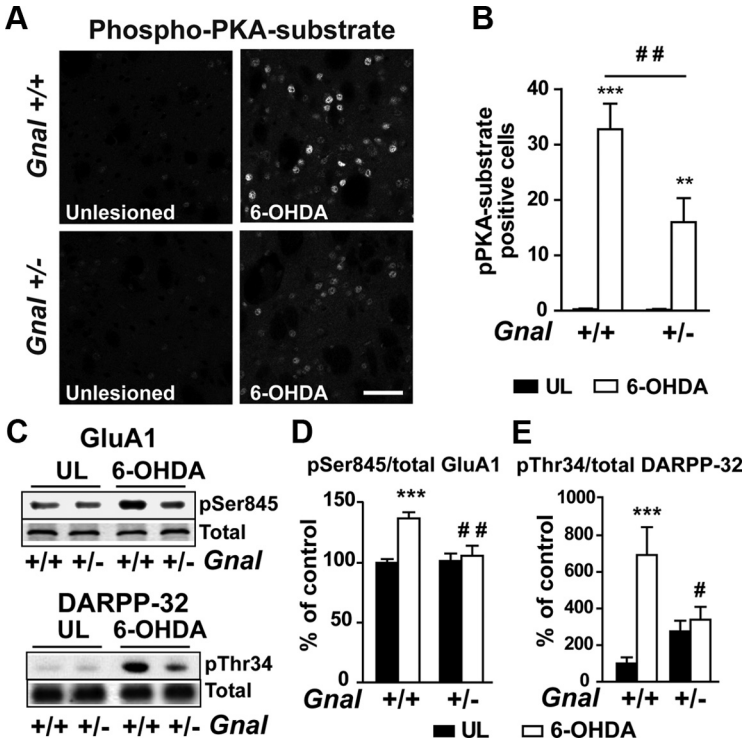

Figure 5. L-DOPA-induced PKA-dependent phosphorylation is markedly impaired in *Gnal* heterozygous mice. ***A***, Single confocal section showing phospho-PKA substrate immunofluorescence in the unlesioned (UL) and 6-OHDA-lesioned dorsal striatum of $Gnal^{+/+}$ (top row) and $Gnal^{+/-}$ (bottom row) mice, 30 min after the last injection of L-DOPA + benserazide. Scale bar, 50 μm. ***B***, Number of phospho-PKA substrate (pPKA substrate)-positive cells in the dorsolateral striatum of wild-type and heterozygous mice. Data are means ± SEM of positive cells in 375 × 375 μm confocal images ($n = 8–11$). Repeated-measures two-way ANOVA (with the within-subjects factor of lesion and the between-subjects factor of genotype): effect of the lesion, $F_{(1,17)} = 54.5$, $p < 0.001$; effect of the genotype, $F_{(1,17)} = 7.04$, $p < 0.02$; and interaction, $F_{(1,17)} = 6.49$, $p < 0.05$. *Post hoc* comparison (Bonferroni's test): $^{**}p < 0.01$and $^{***}p < 0.001$, 6-OHDA versus unlesioned; $^{\#\#}p < 0.01$, $Gnal^{+/-}$ versus $Gnal^{+/+}$. ***C***, Immunoblot analysis using antibodies against phospho-Ser845-GluA1 (pSer845) and total GluA1, phospho-Thr34–DARPP-32 (pThr34), and total DARPP-32 in the unlesioned (UL) and 6-OHDA-lesioned striatum of $Gnal^{+/+}$ and $Gnal^{+/-}$ mice, 30 min after the last injection of L-DOPA + benserazide. ***D***, Quantification of pSer845 normalized to total GluA1, expressed as percentage of unlesioned (UL) striatum of $Gnal^{+/+}$ mice. Data are means ± SEM ($n = 9–15$). Two-way ANOVA: effect of the genotype, $F_{(1,48)} = 6.02$, $p < 0.02$; effect of the lesion, $F_{(1,48)} = 10.8$, $p < 0.01$; interaction, $F_{(1,48)} = 6.8$, $p < 0.05$. *Post hoc* comparison (Bonferroni's test): $^{***}p < 0.001$, 6-OHDA versus unlesioned; $^{\#\#}p < 0.01$, $Gnal^{+/+}$ versus $Gnal^{+/-}$. ***E***, Same representation for pThr34 normalized to total DARPP-32. Data are means ± SEM ($n = 5–9$). Two-way ANOVA: effect of the genotype, $F_{(1,22)} = 1.13$, not significant; effect of the lesion, $F_{(1,22)} = 15.5$, $p < 0.001$; interaction, $F_{(1,22)} = 10.1$, $p < 0.01$. *Post hoc* comparison (Bonferroni's test): $^{***}p < 0.001$, 6-OHDA versus UL; $^{\#}p < 0.05$, $Gnal^{+/+}$ versus $Gnal^{+/-}$.

were stratified on AIM intensity, animals with no or minimal dyskinesia had normal levels of $G\alpha_{olf}$, whereas those with strong dyskinesia had the highest levels. If the degree of D_1R usage was the only factor regulating $G\alpha_{olf}$ levels, their normalization should have been observed in all groups. Therefore, our results, as those in patients (Corvol et al., 2004), suggest the existence of a dysregulation responsible for the "abnormal" persistence of high levels of $G\alpha_{olf}$ and associated with the occurrence of dyskinesia. It should be noted that no persistent increase in $G\alpha_{olf}$ was reported in dyskinetic L-DOPA-treated rats (Rangel-Barajas et al., 2011). We do not know whether this discrepancy results from differences between species or experimental protocols, yet the persistence of $G\alpha_{olf}$ increase in treated PD patients (see above) suggests that results in mice are relevant for the human disease.

$G\alpha_{olf}$ upregulation contributes to the L-DOPA activation of the D_1R/cAMP/PKA pathway in the lesioned striatum

The molecular mechanisms leading to the hypersensitivity of D_1R-stimulated adenylyl-cyclase activity and signaling after DA lesion are unclear because the overall D_1R concentration and its abundance at the plasma membrane are not increased (Savasta et al., 1988; Hervé et al., 1993; Shinotoh et al., 1993; Berthet et al., 2009). Our results strongly support the role of $G\alpha_{olf}$ upregulation in D_1R hypersignaling, because a marked decrease in the PKA-dependent phosphorylations was observed in $Gnal^{+/-}$ mutant mice. L-DOPA-induced phosphorylation was partially (general PKA phosphosubstrates) or massively (phosphorylation of GluA1 or DARPP-32) decreased. Because in mutant mice the levels of $G\alpha_{olf}$ were below those in unlesioned wild-type striatum, we can conclude that the increase in $G\alpha_{olf}$ is critical for D_1R-dependent cAMP/PKA hypersensitivity. These results are in agreement with a previous study showing that the levels of $G\alpha_{olf}$ but not those of D_1R are critical for the efficacy of the D_1R/cAMP/PKA pathway (Corvol et al., 2007). They also account for the increased G-protein activation by D_1R reported in MPTP-lesioned monkeys (Aubert et al., 2005). Additional factors may contribute to the cAMP/PKA hypersensitivity in DA-lesioned striatum, including increased levels of adenylyl-cyclase 5/6 (Rangel-Barajas et al., 2011) or changes in phosphatases or phosphodiesterases levels and/or activities (Meurers et al., 2009).

$G\alpha_{olf}$/cAMP/PKA hypersensitivity does not account for the strong activation of ERK by L-DOPA in dyskinetic animals

In animal models of PD, a strong ERK activation in response to L-DOPA is observed, correlated with the occurrence of LID (Gerfen et al., 2002; Pavón et al., 2006; Santini et al., 2007, 2009b, 2010; Westin et al., 2007; Nicholas et al., 2008; Fasano et al., 2010; Francardo et al., 2011). ERK activation occurs in D_1R-expressing striatonigral neurons (Gerfen et al., 2002; Santini et al., 2009b) and after prolonged treatment in cholinergic interneurons (Ding et al., 2011). The ERK pathway may be important at several levels, including regulation of transcription (Cenci et al., 1998; Aubert et al., 2007) and translation, through the mTORC1 complex (Santini et al., 2009a). The precise molecular mechanism of ERK signaling hypersensitivity is not known. In the present study, despite a dramatic reduction in cAMP/PKA response, the L-DOPA-induced ERK activation was not affected by *Gnal* haplodeficiency. This result strongly suggests that the ERK hyper-responsiveness after DA degeneration does not result from the hypersensitivity of the cAMP/PKA pathway and that the two responses can be dissociated. These results are in line with our previous data on responses to amphetamine in $Gnal^{+/-}$ mice, showing no alteration in the ERK activation despite dramatic reduction in PKA signaling activity (Corvol et al., 2007). A cAMP-independent synergy of D_1R and NMDAR for the ERK activation exists in neurons in culture (Pascoli et al., 2011). *In vivo*, an amplification of this synergy by cAMP/PKA/DARPP-32 appears critical, possibly because of the

high concentrations of regulatory proteins such as DARPP-32 and striatal-enriched tyrosine phosphatase (Valjent et al., 2005). The cause of the D_1R-activated ERK pathway hypersensitivity remains to be identified in DA-lesioned mice but could involve cAMP-independent mechanisms (Gerfen et al., 2008), including crosstalk between D_1R and mGluR5 receptor (Rylander et al., 2009) or dysregulation of protein phosphatases (Meurers et al., 2009). It should be stressed, however, that a basal tonus of cAMP/PKA/DARPP-32 pathway appears required for ERK activation. For instance, the dramatic impairment of the cAMP pathway in *Gnal*$^{-/-}$ homozygous mutants prevented *in vivo* ERK activation by amphetamine (Corvol et al., 2007). In addition, *in vivo* complete inhibition of PKA (Lebel et al., 2010) or genetic deletion of an amplifier of PKA action, DARPP-32 (Santini et al., 2007), decreased the L-DOPA-induced ERK activation in lesioned mice. Accordingly, the existence of a basal level of phospho-DARPP-32 in *Gnal*$^{+/-}$ mice may play a permissive role for ERK activation.

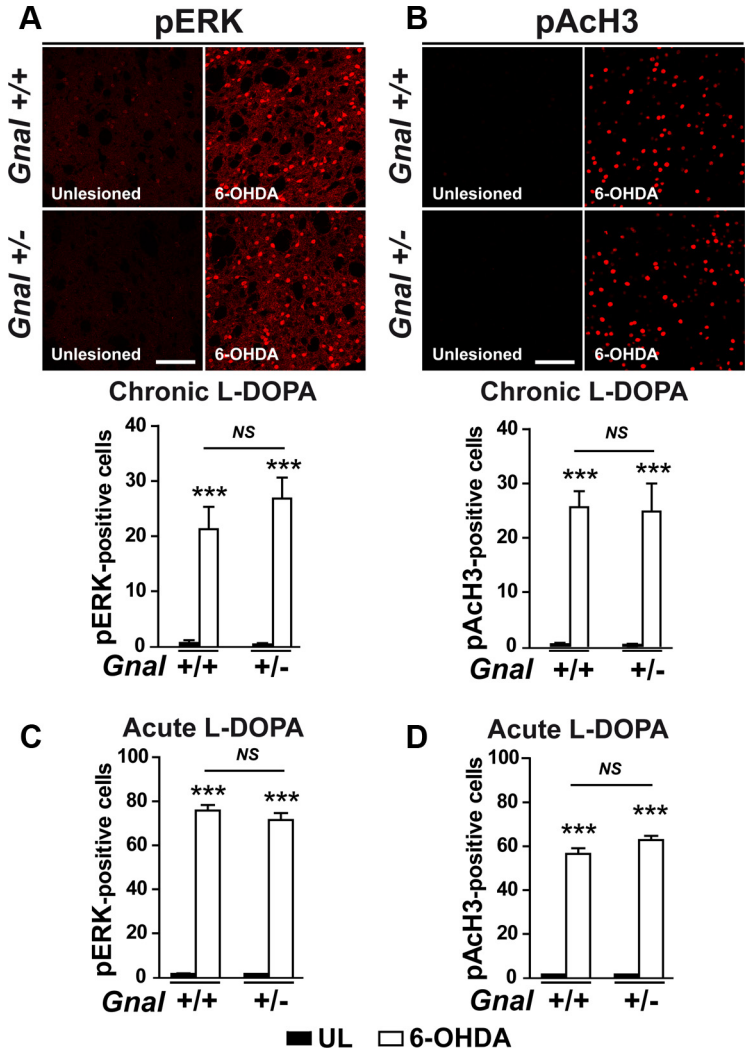

Figure 6. Chronic or acute L-DOPA induces phosphorylation of ERK and histone H3 in the lesioned striatum of *Gnal* heterozygous mice. ***A***, ***B***, Confocal sections through the dorsolateral striatum of unlesioned (UL) and 6-OHDA-lesioned dorsolateral striatum of *Gnal*$^{+/+}$ (top row) and *Gnal*$^{+/-}$ (bottom row) mice, 30 min after the last injection of chronic L-DOPA and benserazide treatment showing phospho-ERK (pERK, ***A***) and phospho-acetyl-histone H3 (pAcH3, ***B***) immunofluorescence. Scale bar, 100 μm. Bottom graphs, Number of pERK- or pAcH3-positive cells in the dorsolateral striatum. Data are means ± SEM in 375 × 375 μm confocal images ($n = 8–11$). Repeated-measures two-way ANOVA (with the within-subjects factor of lesion and the between-subjects factor of genotype): ***A***, pERK, effect of the lesion, $F_{(1,17)} = 67$, $p < 0.0001$; effect of the genotype, $F_{(1,17)} = 0.89$, not significant; interaction, $F_{(1,17)} = 1.03$, not significant; ***B***, pAcH3, effect of lesion, $F_{(1,17)} = 57$, $p < 0.0001$; effect of genotype, $F_{(1,17)} = 0.02$, not significant; interaction, $F_{(1,17)} = 0.01$, not significant. *Post hoc* comparison (Bonferroni's test): ***$p < 0.001$, 6-OHDA versus unlesioned. ***C***, ***D***, Same as in ***A*** and ***B*** but in different groups of mice that received a single injection of L-DOPA ($n = 4–8$ per group). ***C***, pERK, effect of lesion, $F_{(1,20)} = 893$, $p < 0.0001$; effect of genotype, $F_{(1,20)} = 0.79$, not significant; interaction, $F_{(1,20)} = 0.79$; not significant. ***D***, pAcH3, effect of lesion, $F_{(1,20)} = 1231$, $p < 0.0001$; effect of genotype, $F_{(1,20)} = 3.61$, not significant; interaction, $F_{(1,20)} = 3.61$, not significant. *Post hoc* comparison (Bonferroni's test): ***$p < 0.001$, 6-OHDA versus unlesioned.

Hypersensitivity of the D_1R/Gα_{olf}/cAMP pathway is not responsible for dyskinetic behavior but has a permissive role

A variety of dysregulations take place in DA-denervated striatum and are likely to concur to the occurrence of LID (Cenci, 2007; Jenner, 2008; Santini et al., 2008; Calabresi et al., 2010; Feyder et al., 2011; Gerfen and Surmeier, 2011; Murer and Moratalla, 2011). From a therapeutic standpoint, it is important to dissect the mechanisms of induction and expression of LID, which can be targets for potential preventive or symptomatic treatments. Interfering with D_1R (Westin et al., 2007; Darmopil et al., 2009), cAMP/PKA (Lebel et al., 2010), DARPP-32 (Santini et al., 2007; Bateup et al., 2010), Ras-GRF1/ERK (Santini et al., 2007; Fasano et al., 2010), and mTOR (Santini et al., 2009a) decreases or prevents LID. Although these results suggest the involvement of all these signaling modules in the generation of LID, they do not prove that LID results from their upregulation. They only show that their activity is necessary. Our results clarify this situation by showing that LID was still observed in *Gnal*$^{+/-}$ mice despite a marked, but not complete, decrease in D_1R/cAMP/PKA signaling. In addition, in *Gnal*$^{+/-}$ mice, the A_{2A}R/cAMP/PKA signaling is known to be blunted (Corvol et al., 2001; Hervé et al., 2001). A decrease in A_{2A} signaling would be expected to reduce LID development (Xiao et al., 2006), but LID was not decreased in *Gnal*$^{+/-}$ mice. Therefore, we can rule out that increase of cAMP/PKA response is the main culprit for the occurrence of LID. As discussed above for ERK activation, however, cAMP/PKA signaling appears necessary for LID. Indeed, the marked reduction of LID induced by pharmacological inhibition of PKA (Lebel et al., 2010) or by general or targeted DARPP-32 knockout (Santini et al., 2007; Bateup et al., 2010) shows the importance of this pathway. Conversely, our results are compatible with a critical role of ERK in LID generation because its activation was similar in *Gnal*$^{+/-}$ and wild-type mice.

In conclusion, this study allows a better understanding of the importance of various aspects of D_1R signaling hypersensitivity in the generation of LID and their relationships. Our results suggest several important conclusions: (1) Gα_{olf} upregulation is a conserved response to DA lesion, and its persistence during L-DOPA treatment correlates with LID; (2) this upregulation

contributes to the hypersensitivity of the D_1R/cAMP/PKA pathway, which was markedly decreased after reduction in $G\alpha_{olf}$ gene dosage; (3) hypersensitivity of cAMP/PKA signaling does not explain ERK strong activation, which was unaltered in *Gnal* mutant mice; and (4) although the cAMP/PKA pathway is necessary for LID occurrence, its hypersensitivity is unlikely to be its main cause. These results are compatible with a model in which a minimal level of cAMP/PKA pathway is necessary for LID generation, whereas increased ERK signaling may play a direct causal role. Identification of the mechanisms leading to hypersensitivity of the ERK pathway after lesion of DA neurons is therefore an important objective of future studies.

References

Aubert I, Guigoni C, Håkansson K, Li Q, Dovero S, Barthe N, Bioulac BH, Gross CE, Fisone G, Bloch B, Bezard E (2005) Increased D1 dopamine receptor signaling in levodopa-induced dyskinesia. Ann Neurol 57:17–26.

Aubert I, Guigoni C, Li Q, Dovero S, Bioulac BH, Gross CE, Crossman AR, Bloch B, Bezard E (2007) Enhanced preproenkephalin-B-derived opioid transmission in striatum and subthalamic nucleus converges upon globus pallidus internalis in L-3,4-dihydroxyphenylalanine-induced dyskinesia. Biol Psychiatry 61:836–844.

Bateup HS, Santini E, Shen W, Birnbaum S, Valjent E, Surmeier DJ, Fisone G, Nestler EJ, Greengard P (2010) Distinct subclasses of medium spiny neurons differentially regulate striatal motor behaviors. Proc Natl Acad Sci U S A 107:14845–14850.

Belluscio L, Gold GH, Nemes A, Axel R (1998) Mice deficient in G_{olf} are anosmic. Neuron 20:69–81.

Berthet A, Porras G, Doudnikoff E, Stark H, Cador M, Bezard E, Bloch B (2009) Pharmacological analysis demonstrates dramatic alteration of D_1 dopamine receptor neuronal distribution in the rat analog of L-DOPA-induced dyskinesia. J Neurosci 29:4829–4835.

Calabresi P, Di Filippo M, Ghiglieri V, Tambasco N, Picconi B (2010) Levodopa-induced dyskinesias in patients with Parkinson's disease: filling the bench-to-bedside gap. Lancet Neurol 9:1106–1117.

Calon F, Morissette M, Goulet M, Grondin R, Blanchet PJ, Bédard PJ, Di Paolo T (1999) Chronic D1 and D2 dopaminomimetic treatment of MPTP-denervated monkeys: effects on basal ganglia $GABA_A$/benzodiazepine receptor complex and GABA content. Neurochem Int 35:81–91.

Carta AR, Frau L, Lucia F, Pinna A, Annalisa P, Pontis S, Silvia P, Simola N, Nicola S, Schintu N, Nicoletta S, Morelli M, Micaela M (2008) Behavioral and biochemical correlates of the dyskinetic potential of dopaminergic agonists in the 6-OHDA lesioned rat. Synapse 62:524–533.

Cenci MA (2007) Dopamine dysregulation of movement control in L-DOPA -induced dyskinesia. Trends Neurosci 30:236–243.

Cenci MA, Konradi C (2010) Maladaptive striatal plasticity in L-DOPA-induced dyskinesia. Prog Brain Res 183:209–233.

Cenci MA, Lee CS, Björklund A (1998) L-DOPA-induced dyskinesia in the rat is associated with striatal overexpression of prodynorphin- and glutamic acid decarboxylase mRNA. Eur J Neurosci 10:2694–2706.

Corvol JC, Studler JM, Schonn JS, Girault JA, Herv é D (2001) Galpha(olf) is necessary for coupling D1 and A2a receptors to adenylyl cyclase in the striatum. J Neurochem 76:1585–1588.

Corvol JC, Muriel MP, Valjent E, Féger J, Hanoun N, Girault JA, Hirsch EC, Herv é D (2004) Persistent increase in olfactory type G-protein α subunit levels may underlie D_1 receptor functional hypersensitivity in Parkinson disease. J Neurosci 24:7007–7014.

Corvol JC, Valjent E, Pascoli V, Robin A, Stipanovich A, Luedtke RR, Belluscio L, Girault JA, Herv é D (2007) Quantitative changes in Galphaolf protein levels, but not D1 receptor, alter specifically acute responses to psychostimulants. Neuropsychopharmacology 32:1109–1121.

Darmopil S, Martín AB, De Diego IR, Ares S, Moratalla R (2009) Genetic inactivation of dopamine D1 but not D2 receptors inhibits L-DOPA-induced dyskinesia and histone activation. Biol Psychiatry 66:603–613.

Ding Y, Won L, Britt JP, Lim SA, McGehee DS, Kang UJ (2011) Enhanced striatal cholinergic neuronal activity mediates L-DOPA-induced dyskinesia in parkinsonian mice. Proc Natl Acad Sci U S A 108:840–845.

Drinnan SL, Hope BT, Snutch TP, Vincent SR (1991) G_{olf} in the basal ganglia. Mol Cell Neurosci 2:66–70.

Fasano S, Bezard E, D'Antoni A, Francardo V, Indrigo M, Qin L, Dover ó S, Cerovic M, Cenci MA, Brambilla R (2010) Inhibition of Ras-guanine nucleotide-releasing factor 1 (Ras-GRF1) signaling in the striatum reverts motor symptoms associated with L-DOPA-induced dyskinesia. Proc Natl Acad Sci U S A 107:21824–21829.

Feyder M, Bonito-Oliva A, Fisone G (2011) L-DOPA-induced dyskinesia and abnormal signaling in striatal medium spiny neurons: focus on dopamine D1 receptor-mediated transmission. Front Behav Neurosci 5:71.

Francardo V, Recchia A, Popovic N, Andersson D, Nissbrandt H, Cenci MA (2011) Impact of the lesion procedure on the profiles of motor impairment and molecular responsiveness to L-DOPA in the 6-hydroxydopamine mouse model of Parkinson's disease. Neurobiol Dis 42:327–340.

Gerfen CR, Surmeier DJ (2011) Modulation of striatal projection systems by dopamine. Annu Rev Neurosci 34:441–466.

Gerfen CR, Miyachi S, Paletzki R, Brown P (2002) D_1 dopamine receptor supersensitivity in the dopamine-depleted striatum results from a switch in the regulation of ERK1/2/MAP kinase. J Neurosci 22:5042–5054.

Gerfen CR, Paletzki R, Worley P (2008) Differences between dorsal and ventral striatum in Drd1a dopamine receptor coupling of dopamine- and cAMP-regulated phosphoprotein-32 to activation of extracellular signal-regulated kinase. J Neurosci 28:7113–7120.

Girault JA, Raisman-Vozari R, Agid Y, Greengard P (1989) Striatal phosphoproteins in Parkinson disease and progressive supranuclear palsy. Proc Natl Acad Sci U S A 86:2493–2497.

Hemmings HC Jr, Williams KR, Konigsberg WH, Greengard P (1984) DARPP-32, a dopamine- and adenosine 3′:5′-monophosphate-regulated neuronal phosphoprotein. I. Amino acid sequence around the phosphorylated threonine. J Biol Chem 259:14486–14490.

Hervé D, Lévi-Strauss M, Marey-Semper I, Verney C, Tassin JP, Glowinski J, Girault JA (1993) G_{olf} and Gs in rat basal ganglia: possible involvement of G_{olf} in the coupling of dopamine D_1 receptor with adenylyl cyclase. J Neurosci 13:2237–2248.

Hervé D, Le Moine C, Corvol JC, Belluscio L, Ledent C, Fienberg AA, Jaber M, Studler JM, Girault JA (2001) $G\alpha_{olf}$ levels are regulated by receptor usage and control dopamine and adenosine action in the striatum. J Neurosci 21:4390–4399.

Hurley MJ, Mash DC, Jenner P (2001) Dopamine D_1 receptor expression in human basal ganglia and changes in Parkinson's disease. Brain Res Mol Brain Res 87:271–279.

Jenner P (2008) Molecular mechanisms of L-DOPA-induced dyskinesia. Nat Rev Neurosci 9:665–677.

Kull B, Svenningsson P, Fredholm BB (2000) Adenosine A_{2A} receptors are colocalized with and activate g_{olf} in rat striatum. Mol Pharmacol 58:771–777.

Lebel M, Chagniel L, Bureau G, Cyr M (2010) Striatal inhibition of PKA prevents levodopa-induced behavioural and molecular changes in the hemiparkinsonian rat. Neurobiol Dis 38:59–67.

Levis MJ, Bourne HR (1992) Activation of the alpha subunit of Gs in intact cells alters its abundance, rate of degradation, and membrane avidity. J Cell Biol 119:1297–1307.

Lundblad M, Andersson M, Winkler C, Kirik D, Wierup N, Cenci MA (2002) Pharmacological validation of behavioural measures of akinesia and dyskinesia in a rat model of Parkinson's disease. Eur J Neurosci 15:120–132.

Lundblad M, Picconi B, Lindgren H, Cenci MA (2004) A model of L-DOPA-induced dyskinesia in 6-hydroxydopamine lesioned mice: relation to motor and cellular parameters of nigrostriatal function. Neurobiol Dis 16:110–123.

Lundblad M, Usiello A, Carta M, Håkansson K, Fisone G, Cenci MA (2005) Pharmacological validation of a mouse model of L-DOPA-induced dyskinesia. Exp Neurol 194:66–75.

Marcotte ER, Sullivan RM, Mishra RK (1994) Striatal G-proteins: effects of unilateral 6-hydroxydopamine lesions. Neurosci Lett 169:195–198.

Meurers BH, Dziewczapolski G, Shi T, Bittner A, Kamme F, Shults CW (2009) Dopamine depletion induces distinct compensatory gene expression changes in DARPP-32 signal transduction cascades of striatonigral and striatopallidal neurons. J Neurosci 29:6828–6839.

Murer MG, Moratalla R (2011) Striatal signaling in L-DOPA-induced dyskinesia: common mechanisms with drug abuse and long term memory involving D1 dopamine receptor stimulation. Front Neuroanat 5:51.

Nicholas AP, Lubin FD, Hallett PJ, Vattem P, Ravenscroft P, Bezard E, Zhou S, Fox SH, Brotchie JM, Sweatt JD, Standaert DG (2008) Striatal histone modifications in models of levodopa-induced dyskinesia. J Neurochem 106:486–494.

Nishino N, Kitamura N, Hashimoto T, Tanaka C (1993) Transmembrane

signalling systems in the brain of patients with Parkinson's disease. Rev Neurosci 4:213–222.

Pascoli V, Besnard A, Herv é D, Pagès C, Heck N, Girault JA, Caboche J, Vanhoutte P (2011) Cyclic adenosine monophosphate-independent tyrosine phosphorylation of NR2B mediates cocaine-induced extracellular signal-regulated kinase activation. Biol Psychiatry 69:218–227.

Pavón N, Martín AB, Mendialdua A, Moratalla R (2006) ERK phosphorylation and FosB expression are associated with L-DOPA-induced dyskinesia in hemiparkinsonian mice. Biol Psychiatry 59:64–74.

Paxinos G, Franklin KBJ (2001) The mouse brain in stereotaxic coordinates, Ed 2. San Diego: Academic.

Penit-Soria J, Durand C, Besson MJ, Herve D (1997) Levels of stimulatory G protein are increased in the rat striatum after neonatal lesion of dopamine neurons. Neuroreport 8:829–833.

Rangel-Barajas C, Silva I, Lopéz-Santiago LM, Aceves J, Erlij D, Florán B (2011) L-DOPA-induced dyskinesia in hemiparkinsonian rats is associated with up-regulation of adenylyl cyclase type V/VI and increased GABA release in the substantia nigra reticulata. Neurobiol Dis 41:51–61.

Rascol O (2000) Medical treatment of levodopa-induced dyskinesias. Ann Neurol 47:S179–S188.

Rascol O, Nutt JG, Blin O, Goetz CG, Trugman JM, Soubrouillard C, Carter JH, Currie LJ, Fabre N, Thalamas C, Giardina WW, Wright S (2001) Induction by dopamine D1 receptor agonist ABT-431 of dyskinesia similar to levodopa in patients with Parkinson disease. Arch Neurol 58:249–254.

Rascol O, Brooks DJ, Korczyn AD, De Deyn PP, Clarke CE, Lang AE, Abdalla M (2006) Development of dyskinesias in a 5-year trial of ropinirole and L-dopa. Mov Disord 21:1844–1850.

Rylander D, Recchia A, Mela F, Dekundy A, Danysz W, Cenci MA (2009) Pharmacological modulation of glutamate transmission in a rat model of L-DOPA-induced dyskinesia: effects on motor behavior and striatal nuclear signaling. J Pharmacol Exp Ther 330:227–235.

Santini E, Valjent E, Usiello A, Carta M, Borgkvist A, Girault JA, Herv é D, Greengard P, Fisone G (2007) Critical involvement of cAMP/DARPP-32 and extracellular signal-regulated protein kinase signaling in L-DOPA-induced dyskinesia. J Neurosci 27:6995–7005.

Santini E, Valjent E, Fisone G (2008) Parkinson's disease: levodopa-induced dyskinesia and signal transduction. FEBS J 275:1392–1399.

Santini E, Heiman M, Greengard P, Valjent E, Fisone G (2009a) Inhibition of mTOR signaling in Parkinson's disease prevents L-DOPA-induced dyskinesia. Sci Signal 2:ra36.

Santini E, Alcacer C, Cacciatore S, Heiman M, Herv é D, Greengard P, Girault JA, Valjent E, Fisone G (2009b) L-DOPA activates ERK signaling and phosphorylates histone H3 in the striatonigral medium spiny neurons of hemiparkinsonian mice. J Neurochem 108:621–633.

Santini E, Sgambato-Faure V, Li Q, Savasta M, Dovero S, Fisone G, Bezard E (2010) Distinct changes in cAMP and extracellular signal-regulated protein kinase signalling in L-DOPA-induced dyskinesia. PLoS One 5:e12322.

Savasta M, Dubois A, Benavidès J, Scatton B (1988) Different plasticity changes in D1 and D2 receptors in rat striatal subregions following impairment of dopaminergic transmission. Neurosci Lett 85:119–124.

Schwindinger WF, Betz KS, Giger KE, Sabol A, Bronson SK, Robishaw JD (2003) Loss of G protein gamma 7 alters behavior and reduces striatal α_{olf} level and cAMP production. J Biol Chem 278:6575–6579.

Schwindinger WF, Mihalcik LJ, Giger KE, Betz KS, Stauffer AM, Linden J, Herve D, Robishaw JD (2010) Adenosine A2A receptor signaling and golf assembly show a specific requirement for the gamma7 subtype in the striatum. J Biol Chem 285:29787–29796.

Shinotoh H, Inoue O, Hirayama K, Aotsuka A, Asahina M, Suhara T, Yamazaki T, Tateno Y (1993) Dopamine D1 receptors in Parkinson's disease and striatonigral degeneration: a positron emission tomography study. J Neurol Neurosurg Psychiatry 56:467–472.

Sindreu CB, Scheiner ZS, Storm DR (2007) Ca^{2+}-stimulated adenylyl cyclases regulate ERK-dependent activation of MSK1 during fear conditioning. Neuron 53:79–89.

Snyder GL, Allen PB, Fienberg AA, Valle CG, Huganir RL, Nairn AC, Greengard P (2000) Regulation of phosphorylation of the GluR1 AMPA receptor in the neostriatum by dopamine and psychostimulants *in vivo*. J Neurosci 20:4480–4488.

Svenningsson P, Lindskog M, Ledent C, Parmentier M, Greengard P, Fredholm BB, Fisone G (2000) Regulation of the phosphorylation of the dopamine- and cAMP-regulated phosphoprotein of 32 kDa in vivo by dopamine D1, dopamine D2, and adenosine A2A receptors. Proc Natl Acad Sci U S A 97:1856–1860.

Towbin H, Staehelin T, Gordon J (1979) Electrophoretic transfer of proteins from polyacrylamide gels to nitrocellulose sheets: procedure and some applications. Proc Natl Acad Sci U S A 76:4350–4354.

Turjanski N, Lees AJ, Brooks DJ (1997) In vivo studies on striatal dopamine D1 and D2 site binding in L-dopa-treated Parkinson's disease patients with and without dyskinesias. Neurology 49:717–723.

Valjent E, Pagès C, Herv é D, Girault JA, Caboche J (2004) Addictive and non-addictive drugs induce distinct and specific patterns of ERK activation in mouse brain. Eur J Neurosci 19:1826–1836.

Valjent E, Pascoli V, Svenningsson P, Paul S, Enslen H, Corvol JC, Stipanovich A, Caboche J, Lombroso PJ, Nairn AC, Greengard P, Herv é D, Girault JA (2005) Regulation of a protein phosphatase cascade allows convergent dopamine and glutamate signals to activate ERK in the striatum. Proc Natl Acad Sci U S A 102:491–496.

Van Gerpen JA, Kumar N, Bower JH, Weigand S, Ahlskog JE (2006) Levodopa-associated dyskinesia risk among Parkinson disease patients in Olmsted County, Minnesota, 1976–1990. Arch Neurol 63:205–209.

Westin JE, Vercammen L, Strome EM, Konradi C, Cenci MA (2007) Spatiotemporal pattern of striatal ERK1/2 phosphorylation in a rat model of L-DOPA-induced dyskinesia and the role of dopamine D1 receptors. Biol Psychiatry 62:800–810.

Xiao D, Bastia E, Xu YH, Benn CL, Cha JH, Peterson TS, Chen JF, Schwarzschild MA (2006) Forebrain adenosine A2A receptors contribute to L-3,4-dihydroxyphenylalanine-induced dyskinesia in hemiparkinsonian mice. J Neurosci 26:13548–13555.

Zhuang X, Belluscio L, Hen R (2000) $G_{olf}\alpha$ mediates dopamine D_1 receptor signaling. J Neurosci 20:RC91(1–5).